EXPERIMENTAL MEASUREMENTS OF NEUTRINO CROSS-SECTIONS NEAR 1 GEV*

M.O. Wascko

Department of Physics, Imperial College London
Prince Consort Road, London SW7 2AZ, United Kingdom

(Received August 11, 2009)

We summarise recent neutrino and antineutrino measurements near 1 GeV by the K2K, MiniBooNE and SciBooNE collaborations. We focus on experimental methods and note discrepancies between the most commonly used models for neutrino–nucleus interactions and recent high statistics observations of charged-current quasi-elastic scattering as well as charged and neutral current pion production on carbon and oxygen. We discuss possible directions for future measurements.

PACS numbers: 13.15.+g, 25.30.Pt, 95.55.Vj

1. Introduction

Neutrino physics is entering a new era of precision. The need for more precise neutrino cross-section measurements in the 1 GeV region by the next generation of oscillation experiments has been well described [1]. We will not discuss in detail the effects of systematic uncertainties on the next generation of oscillation experiments, but rather focus on recent measurements that have exposed the shortcomings of the current theoretical models describing neutrino–nucleus interactions. We will primarily cover results from the K2K, MiniBooNE and SciBooNE experiments which had been released or presented in public conferences prior to the time of the Lądek School (February, 2009).

In Sec. 1.1, we discuss the past measurements of neutrino interactions near 1 GeV; in Sec. 2 we describe the experiments whose data are shown in later sections; in Sec. 3 we discuss the charged current quasi-elastic (CC QE) process and recent measurements of it; Sec. 4 covers charged-current single

* Presented at the 45th Winter School in Theoretical Physics "Neutrino Interactions: From Theory to Monte Carlo Simulations", Lądek-Zdrój, Poland, February 2–11, 2009.

pion (CC $1\pi^+$) production processes; Sec. 5 covers neutral-current single pion (NC $1\pi^0$) processes; Sec. 6 covers antineutrino measurements and in Sec. 7 we summarise and discuss future directions.

1.1. Previous measurements

Most previous measurements of neutrino interaction cross-sections at these energies were made with bubble chambers exposed to accelerator neutrino beams; the notable exception being the Serpukhov spark chamber. Fig. 1 summarises the past charged-current measurements for both neutrino- and antineutrino–nucleus interactions over a wide range of energies [2]. Bubble chambers offer extremely good final state particle reconstruction resolution, which makes detector systematic uncertainties negligible compared to other sources. However, because events were necessarily reconstructed by hand, all bubble chamber neutrino experiments collected very poor statistics. Lower intensity neutrino beams also contributed to lower statistics.

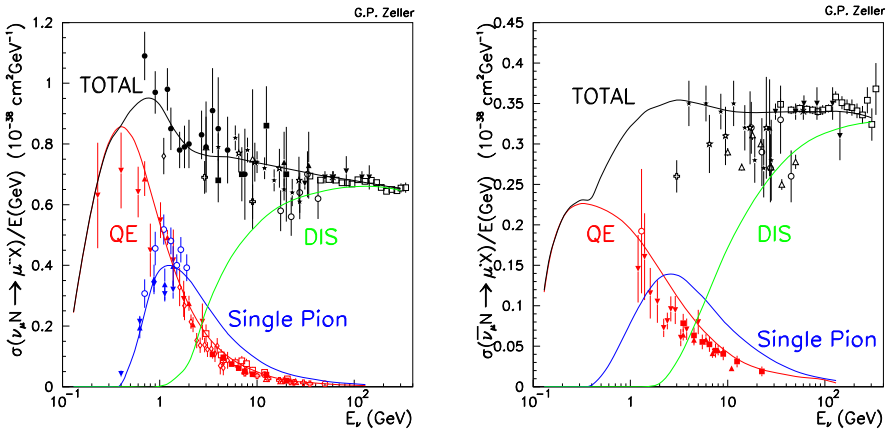

Fig. 1. Past measurements of neutrino (left-hand side) and antineutrino (right-hand side) cross-sections [2].

2. The modern experiments

2.1. Neutrino beam flux predictions

Neutrino cross-section measurements require estimates of the neutrino fluxes; these estimates have proven to be extremely difficult since the advent of accelerator neutrino beams. Most previous experiments perform some calculations of neutrino fluxes based on estimates of the secondary pion spectra; these estimates in the past have had extremely high uncertainties. Because of this, most experiments employed a circular bootstrapping method of estimating the fluxes.

To illustrate the difficulty of estimating neutrino fluxes, Fig. 2 shows four examples of predicted neutrino flux spectra at the MiniBooNE detector [3]. Each flux prediction was produced using exactly the same Monte Carlo (MC) simulation of the neutrino target, horn, and secondary beamline, with the only difference being the primary pion production in each. The largest flux estimate is a factor of four higher than the lowest, illustrating in rather dramatic fashion the difficulty in estimating neutrino fluxes.

Because of the importance of accurate neutrino flux predictions for precise cross-section measurements, several experiments have been performed and planned to make accurate measurements of primary hadron production cross-sections. The HARP experiment at CERN [4] has published precise ($\delta\sigma/\sigma \sim 5\%$) measurements of pion production on an aluminium target at 12 GeV for K2K [5], and pion production on a beryllium target at 8 GeV for the Booster Neutrino Beamline (BNB) [6], as well as others. By explicitly measuring the production of the mesons that contribute to neutrino production, the HARP data solve the problem illustrated in Fig. 2. Flux predictions using the HARP data as input have been used in publications by the K2K, MiniBooNE and SciBooNE collaborations. The MIPP experiment at Fermilab [7] and the NA61/SHINE experiment at CERN [8] have also collected data which should improve the flux predictions for the NuMI beam (MIPP) and T2K (SHINE).

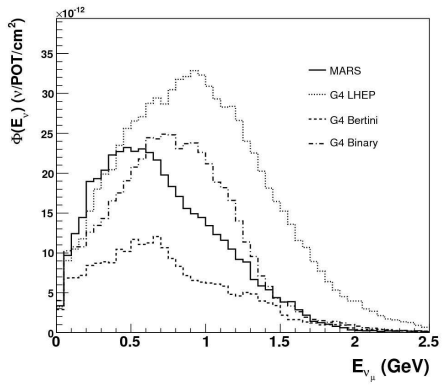

Fig. 2. Four estimates of the neutrino flux at MiniBooNE, using different models for the production of parent-pions by p–Be collisions in the neutrino target [3].

2.2. Neutrino experiments

K2K was a long baseline experiment in Japan which confirmed the atmospheric oscillation signal [9]. MiniBooNE is a short baseline experiment at Fermilab which successfully ruled out the oscillation hypothesis of the LSND signal in neutrinos [10] and is now pursuing a high statistics analysis

of antineutrino data after a preliminary result which showed no evidence of LSND-like oscillations [11]. SciBooNE is a short baseline experiment at Fermilab designed to make precise neutrino and antineutrino cross-section measurements on carbon [12].

K2K is comprised of three main pieces, an accelerator neutrino beam, a near detector suite and a far detector [9]. The neutrino beam is produced by impinging 12 GeV kinetic energy protons on an aluminium target. Secondary charged pions and kaons are bent forward by two toroidal magnetic focussing horns into a 200 m decay volume; the horns increase the neutrino flux in the detector halls by a factor ~ 22. The result is a beam with mean neutrino energy near 1.3 GeV. The neutrinos first pass through the near detectors located 300 m downstream of the neutrino target. The first near detector is a one kiloton water Cherenkov detector (1kT) and the second is a fine-grained detector (FGD) which is comprised of several subsystems: a scintillating fibre detector (SciFi), a lead glass calorimeter (LG), a totally active scintillating bar detector (SciBar) and a muon range detector (MRD). The far detector used for the oscillation analyses is the 50 kiloton water Cherenkov Super Kamiokande detector. K2K took data from June 1999 until November 2004.

MiniBooNE consists of an accelerator neutrino beam and a mineral oil Cherenkov detector. The Booster Neutrino Beam (BNB), which feeds neutrinos to MiniBooNE and SciBooNE, is produced by impinging 8 GeV kinetic energy protons on a beryllium target. The secondary pions and kaons are focused by a single magnetic horn which increases the neutrino flux by a factor ~ 7. The resultant neutrino beam has a mean energy of 0.8 GeV [19]. The polarity of the magnetic horn can be reversed, producing an antineutrino beam with mean energy ~ 0.6 GeV. The MiniBooNE detector is a 0.8 kiloton mineral oil Cherenkov detector located 541 m from the neutrino target [20]. MiniBooNE began collecting beam data in February 2002 and is approved to continue collecting data through at least 2010.

The SciBooNE experiment is a new detector placed in the BNB at 100 m from the neutrino target [12]. The neutrino vertex detector is SciBar, the same fully active scintillating bar detector used in K2K. SciBooNE also uses an electromagnetic calorimeter (EC) placed immediately downstream of SciBar and an MRD that is different from the one used in K2K. SciBooNE took neutrino beam data from June 2007 until August 2008.

Several more experiments have already been running or will be coming on line in the near future to make precise neutrino cross-section measurements. Foremost among these is the MINERνA experiment at Fermilab which started commissioning with neutrino data in the NuMI beamline beginning in April 2009 [13]. MINERνA will have the flexibility of the NuMI beamline allowing it to measure neutrino and antineutrino cross-sections

over a wide range of energies, as well as the capability to change nuclear targets. The MINOS experiment has been running for years in Fermilab's NuMI beamline [14]. Also beginning to take data in 2009 in Fermilab's NuMI beam is Argoneut [15], a liquid argon time projection chamber (LArTPC) which will make new measurements of neutrino cross-sections on argon. The T2K near detectors will be up and running in 2010 affording high statistics neutrino cross-section measurements [16], and the NOνA near detector will make several cross-section measurements [17]. Finally beginning in 2012 the MicroBooNE experiment, a large LArTPC, will begin running in Fermilab's BNB [18].

3. Charged current quasi elastic scattering

The CC QE process, $\nu_\mu n \to \mu^- p$, is important because it is the signal reaction for oscillation experiments in the 1 GeV region. It is used as the signal process because it is the largest neutrino–nucleus cross section below ~ 2 GeV and because the simple final state allows accurate neutrino energy reconstruction using only the measured energy and angle of the outgoing lepton.

The neutrino–nucleon CC QE scattering cross-section is most commonly written according to the Llewellyn-Smith prescription [21], which parameterises the cross section in terms of several form factors which are functions of Q^2, the square of the four-momentum transferred to the nuclear system. Many of the form factors can be taken from electron scattering experiments. However, the axial form factor can only be measured by neutrino scattering. In the past, most experiments have assumed a dipole form for the axial form factor F_A, $F_\mathrm{A}(Q^2) = F_\mathrm{A}(Q^2 = 0)/[1+Q^2/(M_\mathrm{A}^\mathrm{QE})^2]^2$, and used reconstructed Q^2 distributions to extract a value for the axial mass parameter M_A^QE.

To approximate the nuclear environment, the relativistic Fermi gas (RFG) model of Smith and Moniz is used by most experiments [22]. This model assumes that nucleons are quasi-free, with an average binding energy and Fermi momentum which are both specific for particular nuclei. Pauli blocking is included in the model. While such simple models have been demonstrated inadequate for electron scattering experiments, previous neutrino scattering measurements were not sufficient to demonstrate model deficiencies.

More details of the theory of neutrino–nucleus scattering are discussed in detail elsewhere in these proceedings [23].

3.1. K2K SciFi M_A^{QE} analysis

The K2K SciFi group published the first CC QE result at these energies in nearly 20 years [24]. To simulate neutrino–nuclear scattering, K2K uses the NEUT generator MC simulation [25]; for CC QE scattering NEUT uses

the Llewellyn-Smith cross-section with non-dipole vector form factors and the Smith–Moniz RFG model. The SciFi detector is comprised of multiple aluminium modules each containing a network of scintillating fibres in water read out by CCD cameras equipped with image intensifiers. The predominant nuclear target is oxygen. The fibres are oriented in the plane transverse to the neutrino beam direction. Charged particle tracks are detected and their positions and angles reconstructed by collecting light from the fibres in two views ("top" and "side"). Charged current neutrino events are tagged by searching for tracks originating in the SciFi fiducial volume and penetrating into the MRD. The analysis requires that muons stop inside the MRD in order to measure their momenta.

For the CC QE analysis, events are split into three subsamples based on the presence and angle of a second track coming from the neutrino interaction point (defined by the beginning of the muon track). Only one and two track events are used in the analysis. One-track muon events are grouped together; K2K's Monte Carlo (MC) simulation indicates that more than 98% of tagged muon tracks are actually muons [24]. Two-track events are split into two subsamples: a QE-enhanced and a non-QE sample. The QE-enhanced sample is selected by requiring the second track angle be within 25° of the predicted direction based on the observed muon track angle and the assumption that the event was a CC QE interaction ($\Delta\theta_p < 25°$); the non-QE sample is the complement and is used to constrain the backgrounds. Once the samples are defined, the analysers fit for the value of $M_{\mathrm{A}}^{\mathrm{QE}}$ by comparing the reconstructed Q^2 distributions from data with MC simulation. The neutrino energy and momentum transfer are reconstructed using only the observed muon energy and angle under the assumption that the neutrino event was a CC QE interaction.

Figure 3 shows the Q^2 distributions for the three subsamples described above, both data and MC simulation, broken into two experimental configurations. In the K2K-I period, the LG detector was situated between SciFi and the MRD; in the K2K-II period the LG was replaced by SciBar. The data points below 0.2 $(\mathrm{GeV}/c)^2$ are not used in the fit to avoid complications from the effects of the nuclear environment. The extracted value of $M_{\mathrm{A}}^{\mathrm{QE}}$ from the fit is 1.20 ± 0.12 GeV/c^2, which is significantly higher than the average of previous measurements, 1.015 GeV/c^2 [29]. We note that, because of the dipole form, a high value of $M_{\mathrm{A}}^{\mathrm{QE}}$ does not just affect the shape of the Q^2 distribution, it also increases the total rate of CC QE events — which does not conflict with the K2K data.

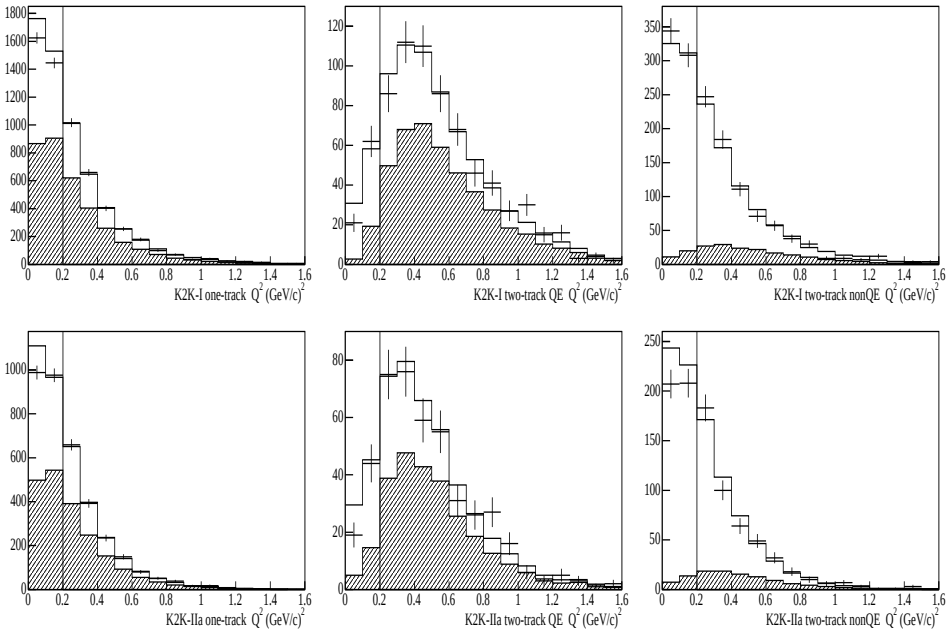

Fig. 3. K2K SciFi CC QE data: reconstructed Q^2 distributions for K2K-1 data (top) and K2K-IIa data (bottom) for the 1-track, 2-track QE enhanced, and 2-track non-QE enhanced samples. The shaded region shows the QE fraction of each sample, estimated from the MC. The lowest two data points in each plot are not included in the fit [24].

3.2. K2K SciBar CC QE analysis

The K2K SciBar CC QE analysis [30] begins in a similar fashion to the SciFi analysis. SciBar was comprised of 64 layers of fully active scintillating strip planes read out by multi-anode photomultipliers (MA-PMTs). Each layer contains two planes of perpendicular strips, with the planes oriented transverse to the neutrino beam direction. Charged-current neutrino events are first selected by matching tracks between SciBar and the MRD. Then the data are split into three samples: one-track, two-track QE enhanced and two-track non-QE. Each event in the two-track QE sample has a second track which satisfies $\Delta\theta_p < 20°$, while the non-QE sample tracks satisfy $\Delta\theta_p > 20°$.

For each event, the values of E_ν and Q^2 assuming a CC QE interaction, are reconstructed. The Q^2 distributions from the three samples are fit simultaneously for the value of $M_{\rm A}^{\rm QE}$. The best fit value is $M_{\rm A}^{\rm QE} = 1.14 \pm 0.077({\rm fit})^{+0.078}_{-0.072}({\rm sys})$ GeV/c^2. This value for $M_{\rm A}^{\rm QE}$uses non-dipole vector form factors; the analysers found that the form of the vector form factors has a significant effect on the extracted value of $M_{\rm A}^{\rm QE}$.

3.3. MiniBooNE CC QE analysis

The MiniBooNE detector is a sphere of mineral oil with 1280 8" PMTs at 575 cm radius facing the centre. The MiniBooNE CC QE analysis [26] begins by selecting clean muon neutrino events, which are identified by observing the muon's Cherenkov ring followed by the Cherenkov ring produced by the decay electron. Requiring the decay electron be located near the end of the reconstructed muon track yields a high purity ν_μCC QE sample. A large fraction of background events are charged current single pion (CC $1\pi^+$), $\nu_\mu N \to \mu^- N \pi^+$, interactions in which the final state pion is not observed. These CC QE-like backgrounds can be constrained with a sample of CC $1\pi^+$ events selected from data by tagging events with two decay electrons [27].

Once the CC QE sample is selected, the analysers examined distributions of the cosine of the muon angle *versus* the muon kinetic energy and found some disagreement in the shapes of the data and MC distributions. MiniBooNE uses the `nuance` [28] neutrino generator MC, which uses the Llewellyn-Smith cross-section with non-dipole vector form factors and the Smith–Moniz RFG model. By plotting the ratio of data over MC, the analysers noted that the shape disagreement between data and MC followed lines on constant Q^2 not lines of constant E_ν. This suggests that the source of the disagreement lay with the cross-section model, not the neutrino flux prediction.

To address the discrepancy, MiniBooNE introduced a new parameter into the Pauli blocking scheme within the Smith–Moniz RFG model. The new parameter, κ, is a scale factor on the lower bound of the nucleon sea and controls the size of the nucleon phase space relevant to Pauli blocking. Then MiniBooNE performed a fit to the reconstructed Q^2 distribution (as in the K2K analyses, both E_ν and Q^2 are reconstructed assuming a CC QE interaction) to extract the value of $M_{\rm A}^{\rm QE}$and κ. The best fit values are $M_{\rm A}^{\rm QE} = 1.23 \pm 0.20$ GeV/c^2 and $\kappa = 1.019 \pm 0.011$.

The effect of the fit is given in Fig. 4. The pre-fit MC curve lies above the data at low Q^2, where Pauli blocking occurs, and below the data at high Q^2. After the fit, the MC agrees the data across the whole range of Q^2. The high value of $M_{\rm A}^{\rm QE}$causes a harder Q^2 spectrum, which improves agreement at high Q^2, and the increased Pauli blocking caused by the high value of κ suppresses production at low Q^2. As mentioned in Sec. 3.1 a high value of $M_{\rm A}^{\rm QE}$also increases the total event rate. Nevertheless the ratio of MiniBooNE's observed CC QE event rate to predicted (using the best fit parameters) is 1.21 ± 0.24 [26].

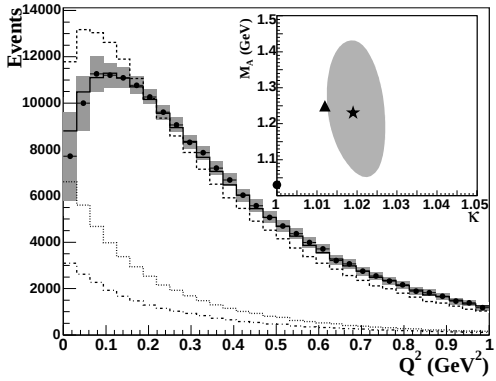

Fig. 4. MiniBooNE CC QE data: reconstructed Q^2 for ν_μCC QE events including systematic errors. The simulation, before (dashed) and after (solid) the fit, is normalised to data. The dotted (dot-dash) curve shows backgrounds that are not CC QE (not "CC QE-like"). The inset shows the 1σ C.L. contour for the best-fit parameters (star), along with the starting values (circle), and fit results after varying the background shape (triangle) [26].

3.4. SciBooNE CC QE analysis

SciBooNE is developing two distinct CC QE data sets, one with tracks matched between SciBar and the MRD and the other with tracks contained within SciBar. To simulate neutrino-nuclear scattering, SciBooNE uses the NEUT generator Monte Carlo (MC) simulation [25].

Charged-current neutrino candidates in the MRD sample are selected by matching tracks originating in the fiducial volume of SciBar and penetrating into the MRD; the muons are tagged by their penetration into the MRD. The upstream end of the muon track defines the neutrino interaction vertex. The analysers separate events based on the number of tracks coming out of the neutrino interaction vertex. One track events have no tracks other than the muon candidate. It was found that there was significant disagreement between data and MC in the $\Delta\theta_p$ distributions, so that parameter was not used to separate signal QE from background non-QE events. Instead, two track events are separated into μ–p and μ–π samples using particle identification based on the energy deposited along the second track. The one-track and μ–p samples are predominantly CC QE events, and the μ–π sample is predominantly CC $1\pi^+$ events. Fig. 5 shows the data and MC distributions for the SciBar-MRD matched sample.

In the SciBar-contained sample, the muons from charged-current neutrino candidates are tagged with particle identification based on energy deposit along the track and by searching for their decay electrons using SciBar's multi-hit TDCs [32]. Events are further classified based on the number and

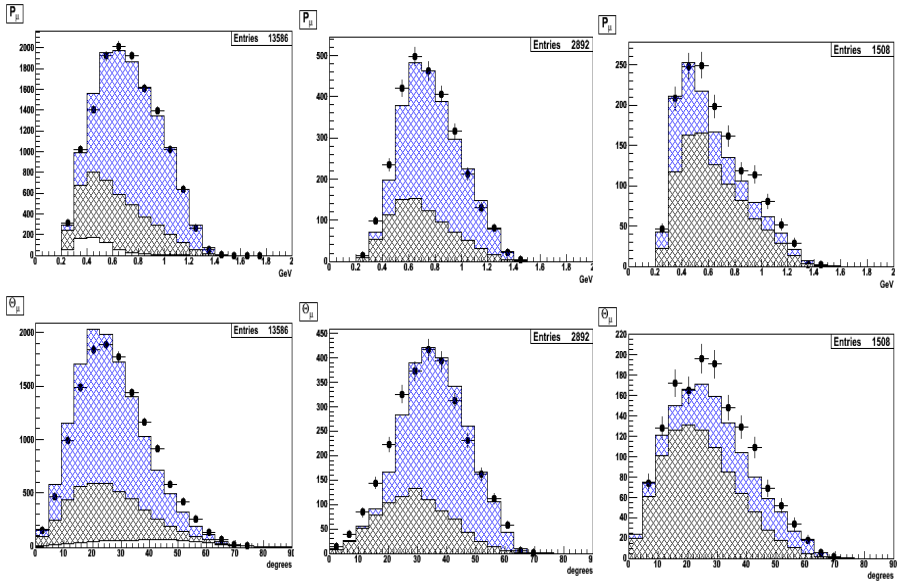

Fig. 5. SciBooNE CC QE data: muon momentum (top) and angles (bottom) for SciBar-MRD matched sample. The left panels show one-track events, the centre panels show two track μ–p events and the right panels show two-track μ–π events. The data (points) include statistical uncertainties only. The MC (histogram) is split into three components: CC QE (blue), non-QE (black) and events originating outside the SciBar fiducial volume (white). The MC was generated with $M_{\rm A}^{\rm QE}$=1.21 GeV/c^2 and is normalised to the MRD-matched data [31].

type of tracks coming from the neutrino vertex. Removing the MRD track-matching cut allows the reconstruction of backwards-going tracks, thus expanding the Q^2 range open to the analysis. The neutrino vertex is defined using the timing of hits within the muon track, and the location of the tagged decay electron. The SciBar contained sample is split into one-track muon events, two track μ–p and two track μ–π events. Fig. 6 shows the data and MC distributions for the SciBar-contained sample.

4. Charged current single pion production

The charged-current single pion (CC $1\pi^+$) production processes, $\nu_\mu N \to \mu^- N \pi^+$, are the second most copious near 1 GeV neutrino energy. They offer rich phenomenology compared to the quasi-elastic process but because there is only one additional final state particle they are simple to tag and reconstruct experimentally. In oscillation experiments they form the primary background channel in ν_μ disappearance searches; the final state pion can

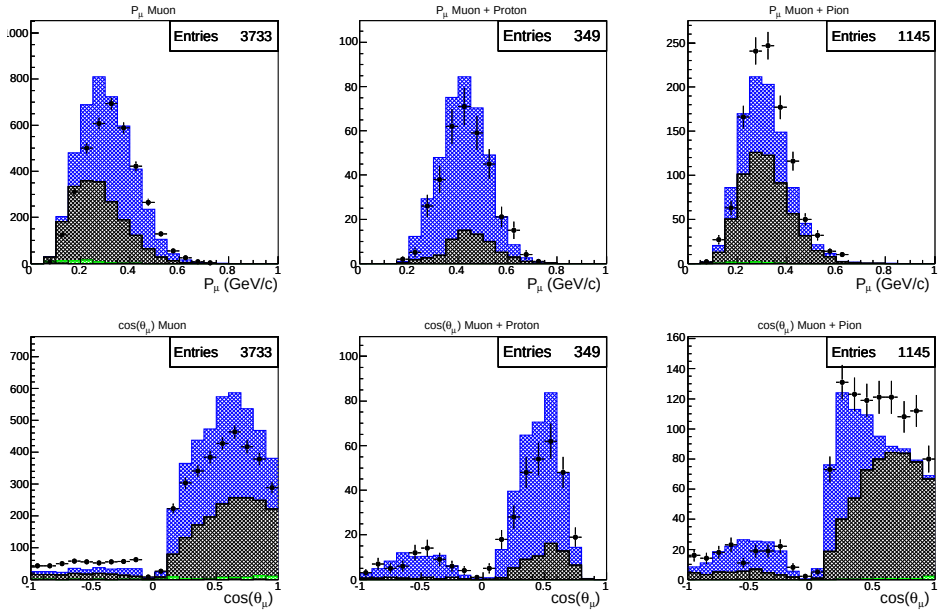

Fig. 6. SciBooNE CC QE data: muon momentum (top) and angles (bottom) for SciBar contained sample. The left panels show one-track events, the centre panels show two track μ–p events and the right panels show two-track μ–π events. The data (points) include statistical uncertainties only. The MC (histogram) is split into three components: CC QE (blue), non-QE (black) and events originating outside the SciBar fiducial volume (green). The MC was generated with $M_{\mathrm{A}}^{\mathrm{QE}}$=1.21 GeV/$c^2$ and is normalised to the SciBar-MRD matched data [31].

be absorbed into the nuclear medium and hence escape observation in the neutrino detector, forming an irreducible background. This phenomenon makes a precise understanding of CC $1\pi^+$ scattering a high priority for the next generation of oscillation experiments [1].

Single pion production on nuclei is often broken into two broad phenomenological categories, coherent and incoherent scattering.

The creation of resonances via interaction of the neutrino with a single nucleon dominates pion production near 1 GeV, and is broadly referred to as incoherent scattering. The most commonly used model for predicting the CC $1\pi^+$ cross-section, and kinematics of final state particles, is the Rein and Sehgal (RS) model [33]. The model is attractive because it describes all neutrino and antineutrino pion production processes in one uniform framework. (The RS model is used to predict neutral current single pion production processes as well.) The model is based on the Feynman, Ravndal and Kislinger [35] relativistic quark oscillator approach and includes the excitations of 18 resonances below hadronic invariant mass 2 GeV/c^2. The model

is parameterised by form factors that are usually assumed to have a dipole form dependent on mass parameters similar to the dipole forms assumed for the axial form factor in CC QE scattering.

Coherent pion production is the interaction of the neutrino with the nucleus as a whole, or in other words with all the nucleons coherently, to produce a pion, $\nu_\mu A \to \mu^- A \pi^+$. The scattering process leaves the nucleus in its ground state, so is an inherently low momentum-transfer process. Again, the most commonly used model to predict the coherent production of pions is the model of Rein and Sehgal [34].

4.1. K2K CC $1\pi^+$ analysis

K2K's CC $1\pi^+$ analysis goal was an extraction of the energy dependent ratio $\sigma_{\mathrm{CC1}\pi}/\sigma_{\mathrm{CCQE}}$ [36]. Again, K2K uses the NEUT MC generator; NEUT models CC $1\pi^+$ interactions using the RS model. The analysis begins with CC neutrino candidates found by matching tracks between SciBar's fiducial

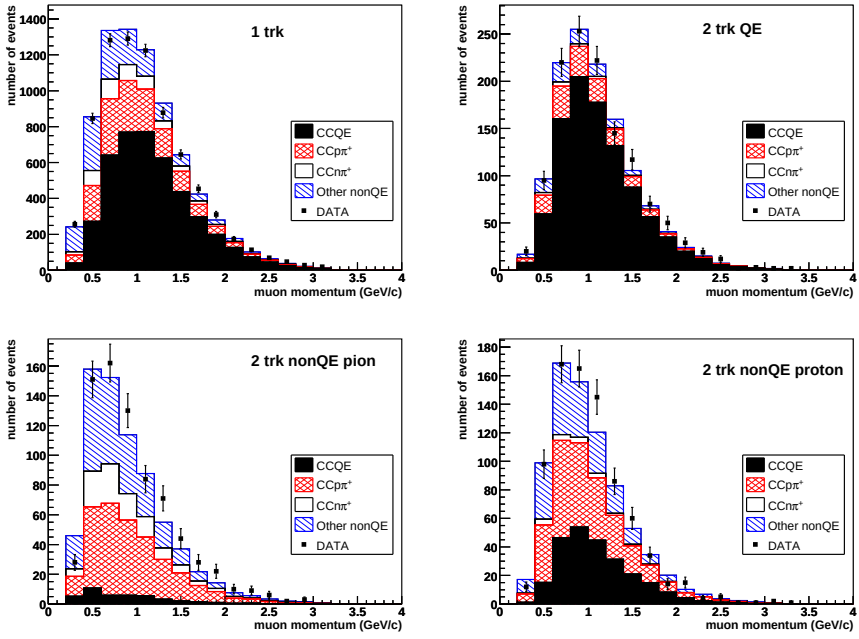

Fig. 7. K2K SciBar CC $1\pi^+$ data; shown are the muon momentum distributions for each of the four data samples used in the analysis. In the top left are the one-track events, in the top right are the two track QE events, in the bottom left are the two track non-QE μ–p events and in the bottom right are the two track non-QE μ–π events. In each panel, the data (black points) are shown with statistical uncertainty, along with CC QE, (black) CC $1\pi^+$ (red and white) and other non-QE (blue) contributions from the MC [36].

volume and the MRD. In such events, the muon is required to stop in the MRD to afford a good muon momentum measurement. The analysis uses one-track and two-track events only. Two track events are split into QE and non-QE samples with a $\Delta\theta_p$ cut at 20°. The non-QE sample is split again into a μ–p and a μ–π sample using particle identification based on energy deposition along the track. The resultant four samples are used to fit for the relative fractions of CC QE, CC $1\pi^+$ and other non-QE events, and thereby extract the cross-section ratio. The muon momentum distributions are shown in Fig. 7.

The analysis proceeds by performing a maximum likelihood fit of the data and MC in bins of p_μ and θ_μ over the four samples simultaneously. The MC is split into four true neutrino energy bins to extract information on the energy dependence of the $\sigma_{\mathrm{CC1}\pi}/\sigma_{\mathrm{CCQE}}$ ratio. The result of the analysis is shown in Fig. 8 (right-hand side) compared with the MiniBooNE and Argonne National Lab [37] $\sigma_{\mathrm{CC1}\pi}/\sigma_{\mathrm{CCQE}}$ results.

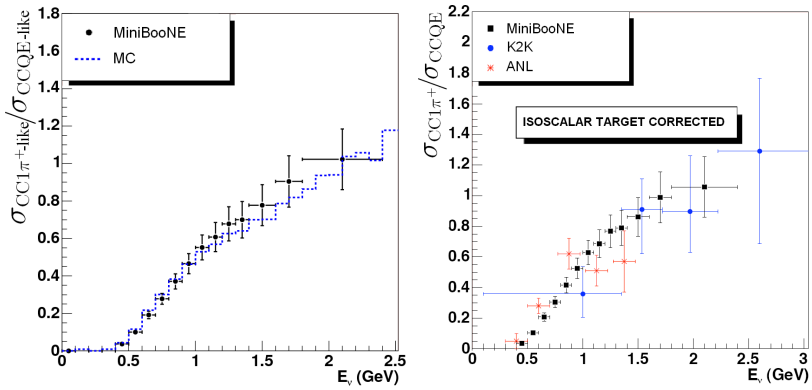

Fig. 8. MiniBooNE CC $1\pi^+$/CC QE ratio measurement (left-hand side) and comparison of MiniBooNE data with results from K2K and ANL [38].

4.2. MiniBooNE CC $1\pi^+$ analysis

As mentioned in Sec. 3.3, MiniBooNE selects a high purity sample of CC $1\pi^+$ events by tagging neutrino events with two decay electrons. Using this simple cut MiniBooNE extracts an high statistics and purity CC $1\pi^+$ data set. The predominant source of Cherenkov light in the MiniBooNE CC $1\pi^+$ events is the μ^-, so the events are fitted with the standard single ring reconstruction algorithm to find E_μ and θ_μ. Those values are used to calculate E_ν and Q^2 assuming CC QE (2 body) kinematics but assuming that the recoiling particle has the mass of the $\Delta(1232)$ resonance instead of the mass of a nucleon. The energy dependent cross-section ratio is calculated directly by using the MiniBooNE CC QE data for the denominator.

MiniBooNE uses the `nuance` MC generator which models CC $1\pi^+$ production using the RS model.

MiniBooNE calculates the cross-section ratio in two ways [38]. The primary measurement is $\sigma_{\text{CC1}\pi\text{-like}}/\sigma_{\text{CCQE-like}}$, a so-called *effective* cross-section ratio. CC $1\pi^+$-like is defined as an event in which exactly one μ^- and one π^+ exit the struck nucleus, and CC QE-like is defined as an event with exactly one μ^- and zero pions. The *effective* CC $1\pi^+$/CC QE ratio is shown in Fig. 8 (left-hand side) as a function of neutrino energy. The secondary MiniBooNE CC $1\pi^+$ measurement is corrected for final state interactions (FSI) — mainly hadronic interactions within the nucleus. The FSI-corrected ratio is shown in Fig. 8 (right-hand side) compared with the results from K2K and ANL. The *effective* ratio does not attempt to make any corrections for nuclear effects and is thus less model-dependent than the FSI-corrected cross-section ratio.

4.3. CC coherent pion production

Noticing that there was disagreement between data and MC in the inelastic CC data samples from their near detector FGDs at low Q^2, and knowing that coherent pion production is an inherently low Q^2 process, the K2K Collaboration was inspired to explore CC coherent pion production with the SciBar detector.

Starting with tracks matched between SciBar and the MRD, the analysers use two-track events to select a sample of CC coherent pions. The two-track sample is split into QE and non-QE samples using a cut on $\Delta\theta_p$ at 25°. The non-QE sample is further refined by using the energy deposited along the track to distinguish μ–p from μ–π events. The analysers tune the MC simulation using the two-track non-QE μ–π data sample, which is enriched with signal events, and the complementary data samples: one-track, two-track QE, and two-track non-QE μ–p , which are all background enriched samples. The tuning is done by fitting the MC reconstructed Q^2 distributions to the data; in all samples Q^2 is reconstructed under the assumption of CC QE kinematics. Once the MC has been tuned, the final event selection cuts are made on the non-QE μ–π sample. Events are required to have forward-going pions. To remove events in which a third particle is emitted but cannot be reconstructed as a track, events are required to have less than 7 MeV *vertex activity:* energy deposited in the scintillator strip which contains the neutrino vertex. The reconstructed Q^2 distributions (data and MC) are shown in Fig. 9 (top). The CC coherent signal sample uses only events with reconstructed Q^2 below 0.1 $(\text{GeV}/c)^2$; as seen in Fig. 9, the K2K data are consistent with the background prediction. The analysers therefore set an upper limit on the CC coherent pion to CC inclusive cross-section ratio, $\sigma(\text{CC coh } \pi)/\sigma(\text{CC inc}) < 0.60 \times 10^{-2}$ at 90% C.L.

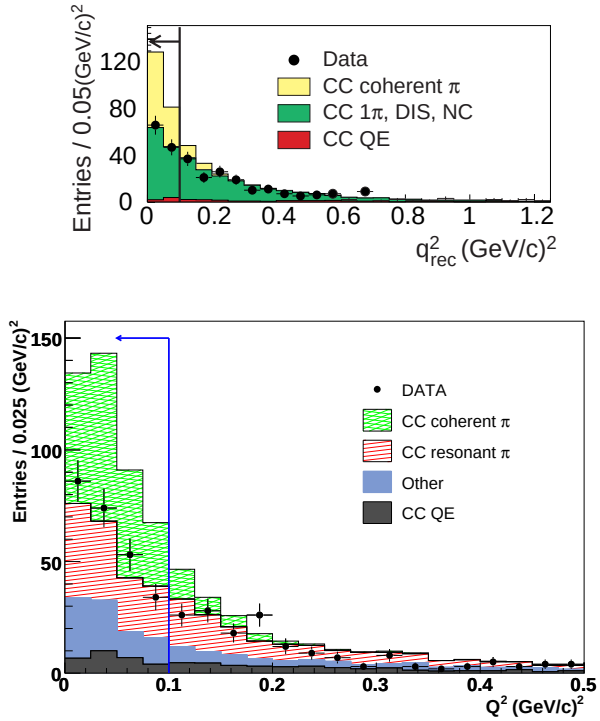

Fig. 9. K2K and SciBooNE neutrino coherent pion search data. Each plot shows reconstructed Q^2 distributions for the coherent pion enhanced samples, which are μ–π non-QE events with low vertex activity. The top panel shows K2K SciBar data and best fit MC [39], and the bottom panel shows SciBooNE data with best fit MC [40].

The SciBooNE CC coherent pion search proceeds along similar lines to the K2K search. Four data samples are selected and used to tune the MC simulation before making the final CC coherent pion event selection [40]. In the SciBooNE analysis, the four samples used to tune the MC are the one-track, two-track μ–p , two-track μ–π with high vertex activity and two-track μ–π with low vertex activity. Again, the MC tuning is done with reconstructed Q^2 distributions. Once the MC is tuned, the final event sample is made by rejecting CC QE events with a $\Delta\theta_p$ cut at 20° and by requiring forward-going pions. The reconstructed Q^2 distributions (data and MC) are shown in Fig. 9 (bottom). The CC coherent signal sample uses only events with reconstructed Q^2 below 0.1 $(\mathrm{GeV}/c)^2$; as seen in Fig. 9, the SciBooNE data are consistent with the background prediction. The analysers therefore set 90% C.L. upper limits on the CC coherent pion to CC inclusive cross-section ratio, $\sigma(\text{CC coh } \pi)/\sigma(\text{CC inc}) < 0.67 \times 10^{-2}$ at 1.1 GeV neutrino energy and $\sigma(\text{CC coh } \pi)/\sigma(\text{CC inc}) < 1.36 \times 10^{-2}$ at 2.2 GeV.

5. Neutral current single pion production

Neutral current π^0 production (NC $1\pi^0$), $\nu_\mu N \to \nu_\mu N \pi^0$, is an important process for experiments searching for $\nu_\mu \to \nu_e$ oscillations because it accounts for the largest single misidentification background. The ν_e background events arise if one of the photons from the π^0 decay is not observed in the neutrino detector or if the photon tracks overlap closely in the lab frame; a single γ (or overlapping γs) creates a shower that is very nearly indistinguishable from a true electron shower in an open volume Cherenkov detector. On the other hand, an open volume Cherenkov detector is quite good for detecting the majority of π^0s produced in its fiducial volume because of the number of radiation lengths of material presented to the decay photons. As we shall see, K2K and MiniBooNE collected remarkably large NC $1\pi^0$ data sets.

NC $1\pi^0$ production cross-sections are typically modeled by experiments using the RS model. Because the neutrino carries away an unknown amount of energy in an NC interaction, the only observables in the detector are the pion and nucleon kinematic variables (although the nucleon is usually not observed).

5.1. K2K NC $1\pi^0$ analysis

K2K used the 1kT water Cherenkov detector to constrain NC $1\pi^0$ production for their ν_e appearance search. NC $1\pi^0$ events are tagged by requiring: no decay electron (which would be observed as a delayed signal); a fully contained event (whose signature is no single PMT with a very high charge hit); two electron-like (showering) rings; and the reconstructed invariant mass, $M_{\gamma\gamma}$, in the range 85–215 MeV/c^2. The analysers measure the rate and momentum spectrum of the π^0s, as well as the NC $1\pi^0$ to CC inclusive cross section ratio. The pion momentum spectrum is shown in Fig. 10 (left-hand side); the measured spectrum is used to tune the MC prediction of π^0 production, which significantly improves the prediction of ν_e background events for the appearance oscillation search. The measured cross-section ratio is $\sigma_{\mathrm{NC}1\pi0}/\sigma_{\mathrm{CC\text{-}inc}} = 0.064 \pm 0.001(\mathrm{stat}) \pm 0.007(\mathrm{syst})$, which agrees well the MC prediction of 0.065 [41].

5.2. MiniBooNE NC $1\pi^0$ analysis

MiniBooNE was designed to search for $\nu_\mu \to \nu_e$ oscillations, so constraining the NC $1\pi^0$ background measurement is a crucial part of the experiment's goals [42]. MiniBooNE analysers select fully contained neutrino candidates with no decay electron. The remaining events are reconstructed according to three separate hypotheses: single muon track, single electron shower and π^0 shower. Likelihood ratios of the three hypotheses are used

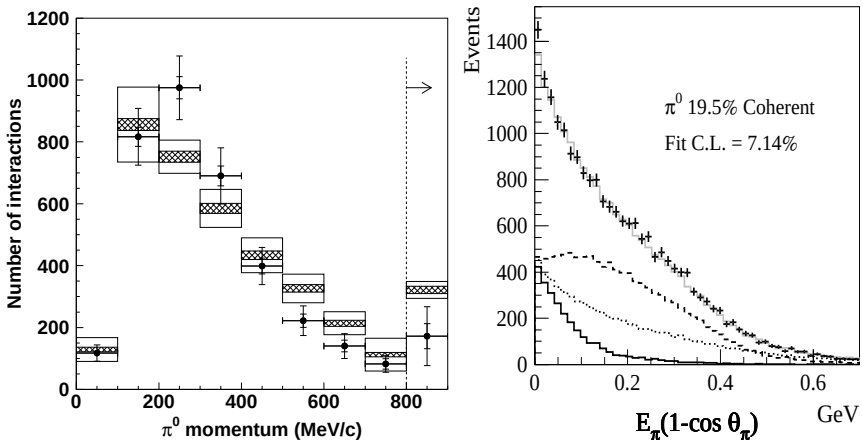

Fig. 10. K2K and MiniBooNE NC $1\pi^0$ data. Left: momentum distribution of K2K NC $1\pi^0$ data (black dots). The inner and outer error bars attached to data points show statistical errors and total errors including systematic errors, respectively. The MC simulation is also shown as a box histogram; the inner boxes represent MC statistical errors and the outer boxes represent the cross-section model uncertainty. Right: energy weighted angular distribution of MiniBooNE data (crosses) and the histograms showing the coherent (solid), resonant (dashed) and background (dotted) contributions as predicted by MC after fitting to the data [41, 42].

as particle identification to select π^0 candidate events. The `nuance` MC simulation used by MiniBooNE models NC $1\pi^0$ production with the RS model, and indicates that the signal to background ratio after the PID cuts is $\sim$30. Next, the analysers require 80 MeV$<M_{\gamma\gamma}<$200 MeV and perform a momentum unsmearing. The extracted pion momentum spectrum is used to tune the MC prediction of the ν_e backgrounds for the oscillation search. MiniBooNE has also measured the coherent fraction via a template fit using MC predicted shapes for the coherent, incoherent (resonant) and other processes in the variable $E_\pi(1-\cos\theta_\pi)$. The results of the fit are shown in Fig. 10 (right-hand side); the extracted coherent fraction observed by MiniBooNE is (19.5$\pm$1.1(stat)$\pm$2.5(syst))% [42].

5.3. SciBooNE NC $1\pi^0$ analysis

SciBooNE begins the NC $1\pi^0$ event selection by requiring two tracks originating in the SciBar fiducial volume disconnected from each other (due to the finite photon conversion distance) with no decay electron tags [43]. The tracks can be contained within SciBar or penetrate into the EC. Particle identification cuts based on energy deposition require electron-like tracks

in SciBar, and if the tracks penetrate into the EC the energy deposit must be shower-like — minimum ionizing particles are rejected. The two tracks are required to point to a common vertex within SciBar to eliminate backgrounds from neutrino interactions upstream of SciBar. Fig. 11 shows the reconstructed pion mass distribution for events contained within SciBar. The analysis is ongoing.

Fig. 11. SciBooNE's reconstructed invariant mass for ν_μNC $1\pi^0$ candidates contained within SciBar [43]. Data (crosses) are shown with statistical errors as well as signal NC $1\pi^0$ (red), internal background (green) and external background (blue) contributions predicted by the MC simulation.

6. Antineutrino cross-section measurements

The search for charge-parity (CP) symmetry violation in the lepton sector is one of the ultimate goals of the worldwide neutrino programme. If the effect is large enough, it could be observed via a difference in the rates of $\nu_\mu \to \nu_e$ and $\overline{\nu}_\mu \to \overline{\nu}_e$ oscillations. However, even the most optimistic scenarios predict that the difference will be relatively small, so the uncertainties on those measurements must also be small. This realisation motivates the need for improved understanding of antineutrino–nucleus cross-section measurements.

Fig. 1 illustrates the paucity of antineutrino cross section measurements at low energy — there are no measurements of any process below 1 GeV. Antineutrino-nucleus cross-sections are significantly smaller — about 50% —

than neutrino–nucleus cross-sections. Moreover, π^+ production in neutrino targets, leading to neutrino flux, is about twice as high as π^- production, leading to antineutrino flux. Together these reductions cause an event rate in antineutrinos that is roughly 25% of the neutrino event rate per proton on target.

6.1. Wrong sign backgrounds

Most accelerator neutrino beams use magnetic focussing horns to increase their neutrino fluxes; reversing the horn's current allows selection of the oppositely charged mesons creating an antineutrino beam. However, paths within the inner conducter of cylindrical horns do not cross any magnetic field lines, so mesons propagating down the center are unaffected. Combined with the fact that π^+ production is far greater than π^- production at the relevant energies, a significant contamination of neutrinos is found in accelerator antineutrino beams. Because they are produced by oppositely charged parent mesons (and will produce oppositely charged leptons in CC interactions) we call these wrong-sign (WS) backgrounds. The magnitude of wrong sign backgrounds in the BNB is illustrated in Fig. 12 [44,45].

When studying the potential for antineutrino running, MiniBooNE developed several techniques to mitigate WS backgrounds [45,46]. These novel techniques are necessary because (current) open volume Cherenkov detectors do not have magnetic fields, so sign selection on an event-by-event basis is impossible. MiniBooNE's WS analysis techniques allow extraction of the total fraction of WS events, but not as a function of energy. MiniBooNE collected antineutrino data from January 2006 until Aug 2007, and then began collecting antineutrino again in April 2008.

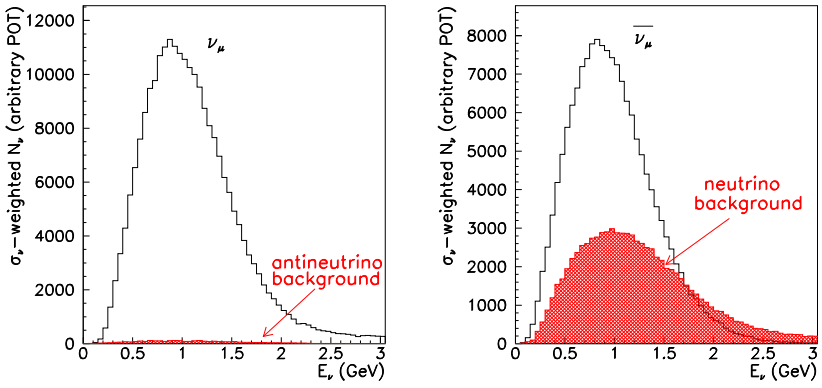

Fig. 12. Monte Carlo simulation of cross-section weighted events in the MiniBooNE detector, showing right sign (black histogram) and wrong sign (red cross-hatched histogram) events. Neutrino mode (left-hand side) and antineutrino mode (right-hand side) spectra are shown [45].

SciBooNE's fine-grained vertex resolution offers a technique not available to MiniBooNE. Whereas neutrino CC QE events, $\nu_\mu n \to \mu^- p$, have two charged particles emerging from the neutrino interaction vertex, antineutrino events, $\overline{\nu}_\mu p \to \mu^+ n$, have just one. So, by simply selecting one-track events, SciBooNE creates a data sample with 80% right sign events; by selecting two-track μ–p events a 70% WS sample is obtained. The results are shown in Fig. 13 [47].

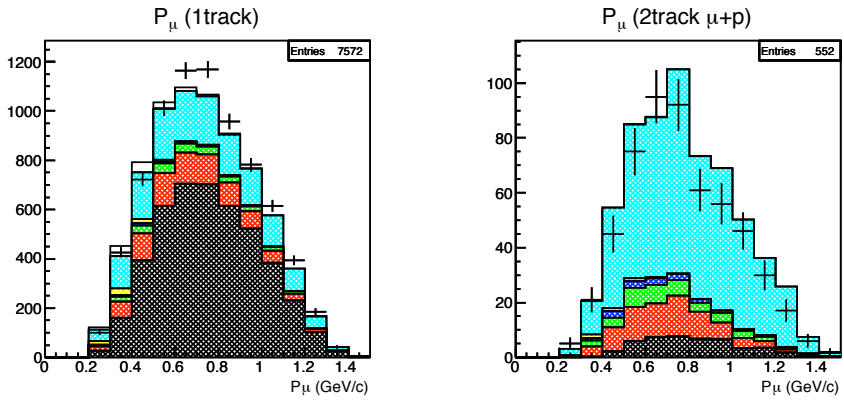

Fig. 13. SciBooNE antineutrino right-sign (left-hand side) and wrong-sign (right-hand side) muon momentum distributions. The data (black points) are shown with statistical uncertainties and MC wrong-sign (cyan) and right-sign (all other colours) contributions are indicated [47].

6.2. SciBooNE $\overline{\nu}_\mu$CC coherent pion search

Charged-current coherent pion production forms a small fraction of CC $1\pi^+$ events, making the coherent pion search essentially an exercise in reducing and constraining backgrounds. Interestingly, most coherent pion production models (including the RS model used by most neutrino generator MCs and experiments) predict that coherent pion production by antineutrinos should have about the same cross-section as production by neutrinos. Thus we can expect that antineutrino searches should be more sensitive since the background rates, per proton on target, will be reduced relative to neutrino searches.

SciBooNE collected antineutrino data from June 2007 until August 2007, and then again from April until August 2008. The SciBooNE antineutrino CC coherent pion search follows the same chain of analysis events as the neutrino search [47]. The coherent pion enriched sample is comprised of two-track, μ–π , low vertex activity, non-QE events with forward going pions.

Then the CC coherent sample is selected by requiring that the reconstructed Q^2 (assuming a CC QE hypothesis) be less than 0.1 GeV^2. The SciBooNE antineutrino CC coherent pion data and MC are shown in Fig. 14.

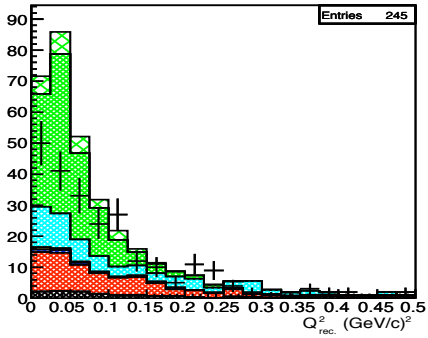

Fig. 14. SciBooNE antineutrino coherent pion sample reconstructed Q^2 distribution. Data (black crosses) are shown with statistical uncertainty, as well as MC CC coherent pion (upper, green area), wrong-sign (middle, cyan area), $\overline{\nu}_\mu$CC QE (lower, red area) and $\overline{\nu}_\mu$CC $1\pi^+$ (incoherent) contributions from the MC [47].

The data clearly lie above the MC predicted backgrounds in the coherent pion region below 0.1 $(\mathrm{GeV}/c)^2$, but the predicted coherent pion signal is larger than what is observed in the data. These preliminary SciBooNE data suggest non-zero coherent pion production, but it appears to be lower than the level predicted by the RS model employed by the NEUT generator. It is interesting to note that if the data excess above the predicted backgrounds were converted into a cross section ratio, it would be consistent with the SciBooNE (and K2K) upper limits observed in the neutrino mode search [47]. Studies are ongoing.

7. Summary and conclusions

The physics of neutrino–nucleus interactions near 1 GeV is today a vibrant field being driven by multiple experiments across the world making new measurements. Although the field lay dormant for nearly 20 years, the recent generation of accelerator neutrino oscillation experiments has revived it with an injection of new, high statistics and high quality data. Recent data from K2K, MiniBooNE and SciBooNE have revealed multiple discrepancies between the industry standard models and new observations. We have summarised the best-studied such discrepancies — those that weigh the heaviest on neutrino oscillation searches. At present there is no clear prescription on which of many possible theory paths forward will yield the best results; in other words there are ample opportunities. By way of summarising, we pose the open questions revealed by the data presented herein.

Why do recent CC QE data near 1 GeV suggest a high value of $M_{\rm A}^{\rm QE}$, and what does such a high value mean? We did not cover it, but at higher energies (3–100 GeV) the NOMAD experiment observes a value of $M_{\rm A}^{\rm QE}$= 1.05±0.02(stat)±0.06(syst) GeV/c^2 [49]. How is this reconciled with the observations from K2K and MiniBooNE?

What is the source of the low Q^2 deficit? This phenomenon has been observed in both CC QE and CC non-QE channels. MiniBooNE addressed the problem by introducing a scaling parameter for Pauli blocking within the context of the RFG model. Colloquially, we can say that MiniBooNE found the RFG model did not have enough knobs to turn so they added one. Why not? Recent work suggests that in the CC $1\pi^+$ channels the low Q^2 issue can be addressed by careful adjustment of the form factors within the RS model [50]. Does the resolution of this issue require better nuclear modeling as well?

How do we reconcile the apparently disparate measurements of coherent pion production in CC and NC channels? Most theoretical models agree on the close relationship between NC and CC coherent pion production but SciBooNE and K2K have set strict limits on the relative amount of CC coherent pion production while MiniBooNE has shown clear evidence for NC coherent pion production. Can the hint that SciBooNE has seen in antineutrino data resolve the issue?

How can we improve the nuclear model used for neutrino scattering? Can we converge on a uniform treatment of final state interactions? Electron scattering experiments have shown conclusively that there are strong intranuclear correlations [51], but the RFG assumes none. Is the low Q^2 issue just a matter of FSI? Very interesting lectures were given in Lądek on these topics [52, 53].

Because of the complexity of testing new models against published data, a new consensus is emerging that we experimentalists must strive to publish POT-normalised differential cross-sections of final state particles. We believe this is the key to reconciling the wealth of new data being collected with the many new theory ideas published in recent years — and we hope that many more new ideas will be inspired by the new data.

May we continue to live in interesting times!

The author would like to sincerely thank the organisers, especially J. Sobczyk, for the invitation to the Lądek school, which was a very stimulating intellectual environment. Dziękuję! Many thanks also go to G.P. Zeller and J. Monroe for many hours of fruitful discussion in the preparation of the lectures and these proceedings.

REFERENCES

[1] T. Itow, *Nucl. Phys. Proc. Suppl.* **3**, 112 (2002); D. Harris, arXiv:hep-ex/0410005v1.

[2] G.P. Zeller, Proceedings of the Venice 2006: Neutrino Oscillartions in Venice, Feb. 2006; G.P. Zeller, NuInt02.

[3] D.W. Schmitz, PhD Thesis, Columbia University, FERMILAB-THESIS 2008-26.

[4] http://harp.web.cern.ch/harp/

[5] M.G. Catanesi, *et al., Nucl. Phys.* **B732**, 1 (2006).

[6] M.G. Catanesi, *et al., Eur. Phys. J.* **C52**, 29 (2007).

[7] http://ppd.fnal.gov/experiments/e907/

[8] https://na61.web.cern.ch/na61/xc/index.html

[9] M.H. Ahn, *Phys. Rev.* **D74**, 072003 (2006).

[10] A.A. Aguilar-Arevalo, *et al., Phys. Rev. Lett.* **98**, 231801 (2007); A.A. Aguilar-Arevalo, *et al., Phys. Rev. Lett.* **102**, 101802 (2009).

[11] A.A. Aguilar-Arevalo, *et al.*, arXiv:0904.1958[hep-ex].

[12] A.A. Aguilar-Arevalo, *et al.*, hep-ex/0601022.

[13] http://minerva.fnal.gov/

[14] http://www-numi.fnal.gov/

[15] http://t962.fnal.gov/

[16] hep-ex/0106019.

[17] http://www-nova.fnal.gov/

[18] http://www-microboone.fnal.gov/

[19] A.A. Aguilar-Arevalo, *et al., Phys. Rev.* **D79**, 072002 (2009).

[20] A.A. Aguilar-Arevalo, *et al., Nucl. Instrum. Methods Phys. Res., Sect.* **A599**, 28 (2009).

[21] C.H. Llewellyn-Smith, *Phys. Rep.* **C3**, 261 (1972).

[22] R.A. Smith, E.J. Moniz, *Nucl. Phys.* **B43**, 605 (1972); Erratum: **B101**, 547 (1975).

[23] J.L. Herraiz, M.C. Martínez, J. Udías, J.A. Caballero, *Acta Phys. Pol. B* **40**, 2405 (2009), this issue.

[24] R. Gran, *et al., Phys. Rev.* **D74**, 052002 (2006).

[25] Y. Hayato, *Nucl. Phys. Proc. Suppl.* **112**, 171 (2002).

[26] A.A. Aguilar-Arevalo, *et al., Phys. Rev. Lett.* **100**, 032301 (2008).

[27] M.O. Wascko, Proceedings of NuInt05, Sept. 2005, hep-ex/0602050.

[28] D. Casper, *Nucl. Phys. Proc. Suppl.* **112**, 161 (2002).

[29] A. Bodek, S. Avvakumov, R. Bradford, H. Budd, *J. Phys. Conf. Ser.* **110**, 082004 (2008).

[30] X. Espinal, F. Sanchez, Proceedings of NuInt07, 2007; doi:10.1063/1.2834461.
[31] J.L. Alcaraz-Aunion, J.J. Walding, Proceedings of NuInt09, May 2009.
[32] H. Takei, Proceedings of NuInt07 2007; doi:10.1063/1.2834504.
[33] D. Rein, L.M. Sehgal, *Ann. Phys.* **133**, 79 (1981).
[34] D. Rein, L.M. Sehgal, *Nucl. Phys.* **B223**, 29 (1983); D. Rein, L.M. Sehgal, *Phys. Lett.* **B657**, (2007).
[35] R.P. Feynman, M. Kislinger, F. Ravandal, *Phys. Rev.* **D3**, (1971).
[36] A. Rodriguez, L. Whitehead, *et. al., Phys. Rev.* **D78**, 032003 (2008).
[37] G.M. Radecky *et al., Phys. Rev.* **D25**, 1161 (1982).
[38] A.A. Aguilar-Arevalo, *et al.*, arXiv:0904.3159[hep-ex].
[39] M. Hasegawa, *et al., Phys. Rev. Lett.* **95**, 252301 (2005).
[40] K. Hiraide, *et al., Phys. Rev.* **D78**, 112004 (2008).
[41] S. Nakayama, C. Mauger, *et al., Phys. Lett.* **B619**, 255 (2005).
[42] A.A. Aguilar-Arevalo, *et al., Phys. Lett.* **B664**, 41 (2008).
[43] Y. Kurimoto, Proceedings of NuInt09, May 2009.
[44] These updated plots are courtesy of G.P. Zeller.
[45] "Addendum to the MiniBooNE Run Plan: MiniBooNE Physics in 2006", MininBooNE Letter of Intenet, 2005.
[46] M.O. Wascko, Proceedings of NuInt05, Sept. 2005, hep-ex/0602051.
[47] H.-K. Tanaka, Proceedings of NuInt09, May 2009.
[48] V. Nguyen, Proceedings of Moriond08, Jan. 2008 arXiv:0806.2347[hep-ex].
[49] V. Lyubushkin, *et al.*, arXiv:0812.4543v3[hep-ex].
[50] J. Nowak, Proceedings of NuInt09, May 2009.
[51] L.B. Weinstein, Proceedings of NuInt07, 2007; doi:10.1063/1.2834517.
[52] S. Dytman, *Acta Phys. Pol. B* **40**, 2445 (2009), this issue.
[53] O. Benhar, *Acta Phys. Pol. B* **40**, 2389 (2009), this issue.